920 *Inorg. Chem.* **1992**, *31*, 920-925

Contribution from the Department of Chemistry and Laboratory for Molecular
Structure and Bonding, Texas A&M University, College Station, Texas 77843

$Mo_2F_4(PR_3)_4$ Compounds and a Comparison of Their Properties with Those of Other $Mo_2X_4(PR_3)_4$ Compounds. A New Synthetic Route to Metal Fluorides by the Reaction of Alkyl Species with Olah's Reagent

F. Albert Cotton* and Kenneth J. Wiesinger†

Received August 22, 1991

The syntheses of $Mo_2F_4(PMe_3)_4$ (**1**) and $Mo_2F_4(PMe_2Ph)_4$ (**2**) from the reaction of $Mo_2Me_4(PR_3)_4$ with Olah's reagent (py·*x*HF) proceed in high yields with the liberation of methane gas. Compound **1** crystallizes in space group $I\bar{4}3m$, with a = 10.8138 (4) Å, V = 1264.5 (2) Å^3, and Z = 2. The molybdenum atoms are disordered over three positions; principal bond distances are Mo(1)-Mo(1)′ = 2.110 (5) Å, Mo(1)-P(1) = 2.444 (3) Å, and Mo(1)-F(1) = 2.105 (2) Å. The new compounds have been characterized by NMR and other spectroscopies, and the properties of **1** have been compared with those of the previously reported $Mo_2X_4(PMe_3)_4$ (X = Cl, Br, I) compounds. Correlations have been found among various physical properties: δ-δ^* and LMCT transitions; Mo-X distances and ionic volume of the halides; atomic number of the halides and NMR shifts.

Introduction

Quadruply bonded dinuclear compounds of the type $Mo_2X_4(PR_3)_4$ are well-known,[1-16] especially for cases where X = Cl, Br, and I. Since 1972,[6] many derivatives of this type have been synthesized and characterized. Entry to the halide species is accomplished by two main synthetic routes:

$$Mo_2(O_2CCH_3)_4 + 4Me_3SiX + 4PR_3 \rightarrow Mo_2X_4(PR_3)_4 + 4Me_3SiO_2CCH_3 \quad (1)$$

$$Mo_2X_8^{4-} + 4PR_3 \rightarrow Mo_2X_4(PR_3)_4 + 4X^- \quad (2)$$

While route 1 is available for X = Cl, Br, I, route 2 is not known for X = I since the $Mo_2I_8^{4-}$ anion remains elusive. Both routes are available for $Mo_2X_4(LL)_2$ complexes where LL = bidentate phosphine. However, no $Mo_2F_4(PR_3)_4$ complexes have been reported to date.

The $Mo_2X_4(PR_3)_4$ complexes have been subjected to extensive study by X-ray crystallography and spectroscopic techniques in order to elucidate their structures, bonding, and electronic relationships. All $Mo_2X_4(PR_3)_4$ (X = halide) compounds have thus far shown eclipsed D_{2d} geometry in the solid state, with Mo-Mo distances of about 2.13 Å. The resonance Raman (rR) spectra consistently show the totally symmetric $\nu_1(Mo_2)$ vibration near 350 cm^{-1};[17] the IR spectra reveal Mo-X bond stretching modes in the region of 350-180 cm^{-1}.

Over the years, there have been attempts in our laboratory and elsewhere to correlate physical properties with one another. In a recent paper we discussed the relationship between the energy of the δ-δ^* transition and the first reduction potential for the $Mo_2X_4(PMe_3)_4$ series where X = NCO, NCS, Cl, Br, and I.[3] Our conclusion was "that the changes in X have little influence on the energy of the HOMO (δ orbital) but, rather, they change the energy of the LUMO (δ^*)". In other studies of the $Mo_2X_4(LL)_4$ compounds,[18-20] we have shown that a linear relationship exists between cos (2χ) (χ = twist angle away from the eclipsed conformation) and the Mo-Mo distance and a relationship exists between the energy of the δ-δ^* transition and cos (2χ). In yet another study,[1] we analyzed the relationship between the energy of the δ-δ^* transition and the π acidities of the PR_3 ligands.

We wish to report here the synthesis and characterization of the first fluoride-containing dimolybdenum quadruply bonded species, namely, $Mo_2F_4(PMe_3)_4$ (**1**) and $Mo_2F_4(PMe_2Ph)_4$ (**2**). In addition, we shall discuss correlations among various physical properties of $Mo_2X_4(PR_3)_4$ compounds such as spectra (δ-δ^*, LMCT), Mo-X distances, ionic volume of the halides, and atomic number of the halides.

Experimental Section

General Procedures. All experiments and manipulations were performed under an atmosphere of dry, oxygen-free argon by the use of standard vacuum-line, Schlenk, and drybox techniques. All glassware was dried at 120 °C for >12 h prior to use. When appropriate, liquid reagents were handled with syringes that were pretreated with suitable solvents.

All solvents were predried over molecular sieves, refluxed over the appropriate drying agent for at least 24 h, and then freshly distilled before use. Toluene, tetrahydrofuran, diethyl ether, and hexanes were dried over a sodium-potassium alloy in the presence of benzophenone.

Reagents. Dimolybdenum(II) tetraacetate[21] and $Mo_2Me_4(PR_3)_4$ compounds[9a] were prepared as reported. Dimethylmagnesium was prepared from the reaction of magnesium metal with dimethylmercury (Alfa) and was then extracted as a diethyl ether solution; its molarity was determined by the method of Bergbreiter,[22] and yields were typically >95%. The phosphines were purchased from Strem and used as received. Olah's reagent, py·*x*HF (70% HF solution), was purchased from PCR and used as received. *Caution*! HF is extremely corrosive to human tissue. An efficient hood and proper protective clothing should be used during experimentation.[23-25]

---

* To whom correspondence should be addressed.

† Research Laboratories, Rohm & Haas Co., Spring House, PA 19477.

(1) Cotton, F. A.; Daniels, L. M.; Powell, G. L.; Kahaian, A. J.; Smith, T. J.; Vogel, E. F. *Inorg. Chim. Acta* **1988**, *144*, 109.

(2) Cotton, F. A.; Extine, M. W.; Felthouse, T. R.; Kolthammer, B. W. S.; Lay, D. G. *J. Am. Chem. Soc.* **1981**, *103*, 4040.

(3) Cotton, F. A.; Matusz, M. *Inorg. Chem.* **1988**, *27*, 2127.

(4) Cotton, F. A.; Poli, R. *Inorg. Chem.* **1987**, *26*, 3228; *J. Am. Chem. Soc.* **1986**, *108*, 5628.

(5) Hopkins, M. D.; Schaefer, W. P.; Bronikowski, M. J.; Woodruff, W. H.; Miskowski, V. M.; Dallinger, R. F.; Gray, H. B. *J. Am. Chem. Soc.* **1987**, *109*, 408.

(6) San Filippo, J., Jr. *Inorg. Chem.* **1972**, *11*, 3140.

(7) San Filippo, J., Jr.; Sniadoch, H. J.; Grayson, R. L. *Inorg. Chem.* **1974**, *13*, 2125.

(8) Glicksman, H. D.; Hamer, A. D.; Smith, T. J.; Walton, R. A. *Inorg. Chem.* **1976**, *15*, 2205.

(9) (a) Cotton, F. A.; Wiesinger, K. J. *Inorg. Chem.* **1990**, *29*, 2594. (b) Girolami, G. S.; Mainz, V. V.; Andersen, R. A.; Vollmer, S. H.; Day, V. W. *J. Am. Chem. Soc.* **1981**, *103*, 3953. (c) Andersen, R. A.; Jones, R. A.; Wilkinson, G. *J. Chem. Soc., Dalton Trans.* **1978**, 446.

(10) Miskowski, V. M.; Goldbeck, R. A.; Kliger, D. S.; Gray, H. B. *Inorg. Chem.* **1979**, *18*, 86.

(11) Cotton, F. A.; Walton, R. A. *Multiple Bonds Between Metal Atoms*; John Wiley & Sons: New York, 1982.

(12) Cotton, F. A.; Wiesinger, K. J. *Inorg. Chem.* **1991**, *30*, 750.

(13) Chisholm, M. H.; Folting, K.; Huffman, J. C.; Tatz, R. J. *J. Am. Chem. Soc.* **1984**, *106*, 1153.

(14) Chisholm, M. H.; Huffman, J. C.; Van Der Sluys, W. G. *J. Am. Chem. Soc.* **1987**, *109*, 2514.

(15) Hopkins, M. D.; Gray, H. B.; Miskowski, V. M. *Polyhedron* **1987**, *6*, 705.

(16) Hopkins, M. D.; Miskowski, V. M.; Gray, H. B. *J. Am. Chem. Soc.* **1988**, *110*, 1787.

(17) San Filippo, J., Jr.; Sniadoch, H. J. *Inorg. Chem.* **1973**, *12*, 2326.

(18) Cotton, F. A.; Powell, G. L. *Inorg. Chem.* **1983**, *22*, 1507.

(19) Campbell, F. L., III; Cotton, F. A.; Powell, G. L. *Inorg. Chem.* **1985**, *24*, 177.

(20) Campbell, F. L., III; Cotton, F. A.; Powell, G. L. *Inorg. Chem.* **1985**, *24*, 4384.

(21) Brignole, A. B.; Cotton, F. A. *Inorg. Synth.* **1972**, *13*, 85.

(22) Bergbreiter, D. E.; Pendergrass, E. *J. Org. Chem.* **1981**, *46*, 219.

(23) Olah, G. A.; Welch, J. T.; Vankar, Y. D.; Nojima, M.; Kerekes, I.; Olah, J. A. *J. Org. Chem.* **1979**, *44*, 3872.

0020-1669/92/1331-0920$03.00/0

Measurements of Physical Properties. NMR spectra were recorded at 22 °C on either a Varian XL-200 spectrometer at 200 MHz for ^1H and 81 MHz for ^{31}P or a Varian XL-400 spectrometer at 376 MHz for ^{19}F and 162 MHz for ^{31}P. Reference standards: ^1H, C_6H_6 (7.15 ppm); ^{19}F, $CF_3C_6H_5$ (−63.75 ppm); ^{31}P, H_3PO_4 (0.00 ppm). UV–visible spectra were recorded on a Cary 17-D spectrophotometer, and IR spectra were recorded as Nujol or Fluorolube mulls on an IBM FTIR-44 spectrophotometer.

The Raman spectra were obtained on an ISA Ramanor 2000 M instrument. The instrument was operated in 2-cm^{-1} steps with slits set at 400 μm. The spectrometer calibration was checked using the spectrum from a neon lamp. Bands are reported accurate to ±4 cm^{-1}. Excitation of the Raman spectra of the samples was done with a Spectra Physics 171 argon laser operated at 514.5 nm and 60-mW power at the sample. Plasma lines were filtered out of the laser beam using an interference filter. The samples were presented to the spectrometer as spinning pellets in an inert-atmosphere cell. The pellets were prepared in a drybox by grinding small amounts of the compounds in potassium fluoride and then pressed in a standard pellet press contained in the drybox followed by loading into the inert-atmosphere cell. No laser damage to the pellets was noted after approximately 3 h in the beam.

Preparation of $Mo_2F_4(PMe_3)_4$ (1). $Mo_2Me_4(PMe_3)_4$ was prepared from $Mo_2(O_2CCH_3)_4$ (0.500-g scale).[9a] However, the solid was not isolated; instead, the deep blue hexane solution was cooled to 0 °C. To this vigorously stirred solution were added PMe_3 (0.10 mL) and then py·*x*HF (Olah's reagent, 70% HF, 0.120 mL) which resulted in an immediate but gentle evolution of gas. Over the course of several minutes, the gas evolution diminished and the solution took on a burgundy-red color. The cold-temperature bath was removed, and stirring of the solution was continued at 25 °C for 2 h. All volatiles were removed by vacuum distillation to give a dark burgundy-red residue. The trap was charged with anhydrous KF to capture any residual HF gas. It is of extreme importance to pump on the dry residue for at least 2 h in order to remove all PMe_3 and HF, which apparently form $[HPMe_3]F$ during the course of the reaction. If the dark burgundy-red residue is not dried long enough, a greenish-brown solid results later during volume reduction. The composition of the green-brown material has not yet been established. The dark burgundy-red residue was extracted with hexanes (45 mL), and the extract was filtered through Celite. The resulting solution was reduced in volume to about 7 mL and then cooled to 0 °C to obtain crystals suitable for X-ray diffraction. In a similar experiment, all the volatiles were removed to provide 480 mg (70% yield) of a deep burgundy-red microcrystalline material. The rR spectrum showed a strong band at 354 cm^{-1} followed by overtones out to $4\nu_1$. The IR bands were as follows (cm^{-1}): 1780 w, 1720 m, 1601 w, 1277 m, 1260 w, 1015 w, 955 vs, 855 m, 850 m, 803 m, br, 740 s, 732 s, 668 m, 502 vs, 457 vs, 333 m, br, 248 m, sharp. UV–vis (benzene, nm): 550, 417, 283. NMR (C_6D_6, ppm): ^1H, 1.43, virtual triplet; ^{19}F, −216.0, virtual triplet; ^{31}P, −8.72, m.

Preparation of $Mo_2F_4(PMe_2Ph)_4$ (2). $Mo_2Me_4(PMe_2Ph)_4$ was prepared from $Mo_2(O_2CCH_3)_4$ (0.500-g scale).[9a] The reaction was performed in an analogous fashion to that for **1**, except that the hexanes were replaced by toluene. After the reaction was complete and all volatiles were removed, the burgundy-colored residue was extracted with a hexane/toluene solution (1:1, 40 mL). The resulting solution was filtered through Celite, and all volatiles were removed to yield 474 mg of a dark burgundy-colored solid. The rR spectrum showed a strong band at 342 cm^{-1}, again followed by overtones out to $4\nu_1$. UV–vis (benzene, nm): 566. NMR (C_6D_6, ppm): ^1H, 7.16–7.61, m, 1.84, virtual triplet; ^{19}F, −196.9, virtual triplet; ^{31}P, −0.004, m.

Table I. Crystal Data for $Mo_2F_4(PMe_3)_4$ (**1**)

formula	$Mo_2P_4F_4C_{12}H_{36}$
fw	572.19
space group	$I\bar{4}3m$
$a = b = c$, Å	10.8138 (4)
$\alpha = \beta = \gamma$, deg	90.00
V, Å^3	1264.5 (2)
Z	2
d_{calc}, g/cm^3	1.503
cryst size, mm	0.30 × 0.25 × 0.14
μ(Mo Kα), cm^{-1}	12.405
data collection instrument	Enraf-Nonius CAD-4
radiation monochromated	Mo Kα (λ = 0.71073 Å)
orientation reflns: no.; range	25; $20 < 2\theta < 32$
temp, °C	−60
scan method	ω–2θ
data collection range (2θ), deg	$4 < 2\theta < 55$
no. of unique data; total with $F_o^2 > 3\sigma(F_o^2)$	4; 117
no. of params refined	17
transm factors: max; min	1.00; 0.82
R^a	0.0627
R_w^b	0.0888
quality of fit indicator[c]	2.34
largest shift/esd, final cycle	0.01
largest peak, e/Å^3	0.548

[a] $R = \sum||F_o| - |F_c||/\sum|F_o|$. [b] $R_w = [\sum w(|F_o| - |F_c|)^2/\sum w|F_o|^2]^{1/2}$; $w = 1/\sigma^2(|F_o|)$. [c] Quality-of-fit $= [\sum w(|F_o| - |F_c|)^2/(N_{observns} - N_{params})]^{1/2}$.

Table II. Positional Parameters and Equivalent Isotropic Thermal Parameters (Å^2) and Their Estimated Standard Deviations for $Mo_2F_4(PMe_3)_4$ (**1**)

atom	x	y	z	B^a
Mo(1)	0.0976 (3)	0.000	0.000	4.13 (4)
P(1)	−0.1546 (3)	$-x$	$-x$	6.07 (3)
F(1)	0.135 (1)	$-x$	$-x$	11.3 (2)
C(1)	−0.138 (2)	$-x$	0.322 (1)	12.5 (4)

[a] Anisotropically refined atoms are given in the form of the equivalent isotropic displacement parameter defined as $(4/3)[a^2\beta_{11} + b^2\beta_{22} + c^2\beta_{33} + ab(\cos\gamma)\beta_{12} + ac(\cos\beta)\beta_{13} + bc(\cos\alpha)\beta_{23}]$.

Table III. Selected Bond Distances (Å) and Angles (deg) for $Mo_2F_4(PMe_3)_4$ (**1**)[a]

Distances			
Mo(1)′–Mo(1)	2.110 (5)	Mo(1)–F(1)	2.105 (2)
Mo(1)–P(1)	2.444 (3)	P(1)–C(1)	1.83 (1)
Angles			
Mo(1)′–Mo(1)–P(1)	104.63 (8)	Mo(1)–P(1)–C(1)	125.7 (5)
Mo(1)′–Mo(1)–F(1)	101.1 (3)	Mo(1)–P(1)–C(1)′	96.5 (4)
P(1)′–Mo(1)–P(1)	150.7 (2)	Mo(1)–P(1)–C(1)″	125.7 (5)
P(1)–Mo(1)–F(1)	87.2 (1)	C(1)′–Mo(1)–C(1)	100.9 (1)
F(1)′–Mo(1)–F(1)	157.8 (4)		

[a] Numbers in parentheses are estimated standard deviations in the least significant digits.

X-ray Diffraction Methods for $Mo_2F_4(PMe_3)_4$ (1)

Crystals were grown as described. The crystals were handled in a mineral oil/solvent mixture, examined under the microscope, and cut to the appropriate size. The crystals did not extinguish under polarized light, but appeared to be of good quality when they were examined by microscope under high magnification. One crystal was mounted on a quartz fiber with Apiezon T stopcock grease and immediately transferred to the cold stream of nitrogen (−60 °C) on the Enraf-Nonius CAD-4 diffractometer.

After the normal procedures, 25 reflections were found, centered, and indexed to give a body-centered cubic unit cell. Axial photographs, as well as photographs of the face and the body diagonals, supported the assignment of body centering and indicated that the Laue class was $m3m$. The data were collected with the collection range starting at (000) and continuing to (*hkl*) for absolute *h* > absolute *k*. No decay was observed from the monitoring of three intensity standards which were observed every hour. The data were corrected for absorption by using azimuthal scans of seven reflections with Eulerian angle of χ near 90°.[26,27]

The systematic absences along with the Laue class allowed three possible space groups: $I432$ (No. 211), $I\bar{4}3m$ (No. 217), and $Im\bar{3}m$ (No. 229). The structure of $Mo_2Cl_4(PEt_3)_4$, previously determined in our laboratory,[1] was solved and refined in space group $I\bar{4}3m$ (No. 217). It seemed reasonable to us that these two compounds might crystallize in the same space group and orientation. The refinement was begun by calculating the position of the Mo atom with the assumption that the Mo–Mo distance was 2.10 Å and that it was located at the position (x, 0, 0). This model refined to only 51%, although the position and thermal parameters were steady. The phosphorus and fluorine atomic positions were calculated by assuming that the atoms were located at (x, $-x$, $-x$), analogous to those in $Mo_2Cl_4(PEt_3)_4$. After several full-matrix cycles,

---

(24) Olah, G. A.; Watkins, M. *Org. Synth.* **1978**, *58*, 75.

(25) Sharts, C. M.; Sheppard, W. A. *Org. React.* **1974**, *21*, 192, 220.

(26) Bino, A.; Cotton, F. A.; Fanwick, P. E. *Inorg. Chem.* **1979**, *18*, 3558.

(27) North, A. C. T.; Phillips, D. C.; Matthews, F. S. *Acta Crystallogr.* **1968**, *A24*, 351.

the residuals converged to $R = 18.4\%$ and $R_w = 25.9\%$. A difference Fourier map revealed the location of the carbon atom; with all atoms isotropic, the residuals converged at $R = 15.1\%$ and $R_w = 25.0\%$. The model converged to $R = 6.27\%$ and $R_w = 8.188\%$ with all atoms [Mo(1), P(1), F(1), and C(1)] anisotropic. The other possible space groups gave no solutions.

Final residuals and figures of merit as well as crystal data collection parameters are reported in Table I. Positional and equivalent isotropic thermal parameters are listed in Table II. Selected bond distances and bond angles are listed in Table III.

Results and Discussion

Synthesis. The search for a synthetic route to $Mo_2F_4(PR_3)_4$ compounds had perplexed us for some time. Our early efforts were directed toward, though not limited to, the conversion of $Mo_2Cl_4(PR_3)_4$ and $Mo_2(O_2CCR_3)_4$ to $Mo_2F_4(PR_3)_4$ and $Mo_2F_8^{4-}$ species. Several papers of possible use to us have appeared on the properties and uses of fluoride reagents.[28-31] Reactions of $Mo_2Cl_4(PR_3)_4$ with the "naked" fluoride[30,31] of various MF·crown ether (M = Li, Na, K) reagents in a number of solvents have been fruitless, as only the starting materials persisted. Since BaF_2 is slightly soluble in alcohols and $BaF_2{\cdot}BaX_2$ (X = Cl, Br, I) are not, we were surprised that the reaction between $Mo_2Cl_4(PR_3)_4$ and BaF_2 again resulted in the persistence of the starting materials. The reaction of $Bu^n{}_4NF{\cdot}3H_2O$, $Mo_2(O_2CCH_3)_4$, and PMe_3 in THF gave an orange-red solution within several hours, which may have contained the axially coordinated $Mo_2(O_2CCH_3)_4(PMe_3)_2$ or $[Bu^n{}_4N]_x[Mo_2(O_2CCH_3)_4F_x]$ with $x = 1$ or 2. However, the reaction solution slowly decomposed to a dark intractable material as gas bubbles appeared in the reaction solution.

In a recent paper,[32] the definitive isolation of a soluble, water- and HF-free source of fluoride, NMe_4F, was reported along with a thorough analysis of the background literature. We are currently investigating the use of this reagent in our continuing efforts to prepare $Mo_2F_8^{4-}$ species. We have also reacted Olah's reagent[23,24] with both $Mo_2Cl_4(PR_3)_4$ and $Mo_2(O_2CCH_3)_4$ in efforts to synthesize $Mo_2F_8^{4-}$ or $Mo_2F_4(PR_3)_4$ species; all attempts have thus far proved futile.

It seems that the key to this chemistry is the availability of a reactive F^- source in concert with the proper solvents and reaction conditions. We are puzzled by the failure of some of the above mentioned reactions, since they have been successful for similar systems. Nonetheless, efforts are continuing along these lines and we are also considering the use of $Mo_2F_6(py)_4$, which was recently reported.[33]

Contrary to Wilkinson's report,[9c] $Mo_2Me_4(PR_3)_4$ compounds react with CF_3CO_2H and alcohols to give $Mo_2(O_2CCF_3)_4(PR_3)_2$ and $Mo_2(OR')_4(PR_3)_4$, respectively. More importantly, $Mo_2Me_4(PMe_3)_4$ reacts with pentafluorophenol to produce $Mo_2(OC_6F_5)_4(PMe_3)_4$.[12] Furthermore, we report here that Olah's reagent (py·*x*HF, 70% HF solution) reacts quickly and efficiently with $Mo_2Me_4(PR_3)_4$ compounds to give $Mo_2F_4(PMe_3)_4$ (**1**) and $Mo_2F_4(PMe_2Ph)_4$ (**2**). In all cases, methane gas is evolved, and this evidently provides the driving force for the reactions.

The synthesis we are reporting is in many ways simple and straightforward, although it is important to use great caution when handling Olah's reagent.[23-25] The reaction proceeds in high yield and purity, but only when the product is thoroughly dried before the final extraction and filtering procedure. It is convenient to use the $Mo_2Me_4(PR_3)_4$ starting material in situ, rather than to isolate it. This method typically gives a much higher yield and obviously saves time.

The stabilities of solutions of **1** and **2** require some comment. The solutions seem to be light sensitive. When two identical solutions were stored at room temperature, the one exposed to light decomposed within 48 h; the other solution whose Schlenk tube had been completely wrapped in aluminum foil was stable for more than 1 week. Furthermore, stability of the compounds in solution appears to increase with the length of drying time as mentioned above.

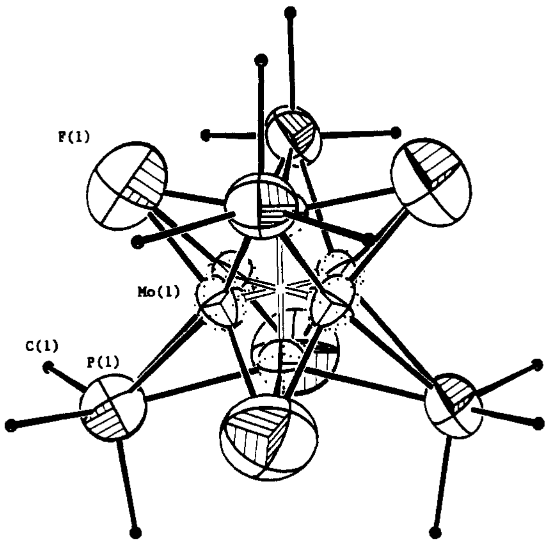

Figure 1. ORTEP drawing of $Mo_2F_4(PMe_3)_4$ (**1**), showing the 3-fold disorder of the molybdenum atoms.

Table IV. Selected Physical Properties of $Mo_2X_4(PMe_3)_4$ Complexes

property	F	Cl	Br	I
δ–δ^*, nm	550	580	598	633
ϵ_{max}, $M^{-1}\ cm^{-1}$	2090	3110	4060	5250
LMCT, nm	283	324	345	395
ϵ_{max}, $M^{-1}\ cm^{-1}$	2110	3720	6650	11850
^1H NMR, ppm	1.43	1.47	1.57	1.76
^{31}P NMR, ppm	−8.72	−9.27	−11.45	−14.98
Mo–X, Å	2.105 (2)	2.414 [1]	2.549 [2]	2.759 [3]
Mo–P, Å	2.444 (3)	2.545 [1]	2.546 [6]	2.562 [5]
Mo–Mo, Å	2.110 (5)	2.130 (0)	2.125 (1)	2.129 (1)
Mo–Mo–P, deg	104.63 (8)	102.3 (1)	102.8 (1)	104.54 [6]
Mo–Mo–X, deg	101.1 (3)	112.2 (1)	113.5 (1)	113.73 [4]
V_{ionic}, Å^3	9.86	26.09	31.54	44.60
atomic no.	9	17	35	53
X radius (covalent), Å	0.72	0.99	1.14	1.33
Mo radius (calc), Å	1.385	1.424	1.409	1.429

The ^{19}F and $^{31}P\{^1H\}$ NMR spectra of **1** and **2** are complex, owing to the very large number of distinct coupling constants (in spite of the fact that symmetry makes all four nuclei of each type equivalent). The two spin systems (^{19}F, ^{31}P) are each of the $AA'A''_2XX'X''_2$ type, for which there is no published analysis that we know of. Each may be expected to show the effects of homo- as well as heteronuclear couplings, and thus they need not (and do not) display the same fine structure. Since we cannot anticipate any chemically or theoretically useful benefit from a complete analysis of these spectra (nor have we obtained them under optimum resolution), we have made no attempt to carry out such analyses. It may be noted that Chisholm and co-workers[34] reported the spectrum of $Mo_2F_2(OBu^t)_4(PMe_3)_2$ and obtained a computer simulation in which P–P, F–F, and P–F coupling constants were all included.

Molecular Structure of $Mo_2F_4(PMe_3)_4$ (1). The molecular structure of **1** is typical for $Mo_2X_4(PMe_3)_4$ complexes, with D_{2d} geometry as shown in Figure 1. In the cubic crystal, the dimolybdenum core is disordered in three directions although the F and PMe_3 ligands occupy separate sites. The three Mo–Mo orientations, each with $^1/_3$ occupancy, coincide with the *x*, *y*, and *z* directions of the unit cell. This is the first case among all $Mo_2X_4(PMe_3)_4$ compounds (X = Cl, Br, I, Me_3, NCO, NCS) in

---

(28) Clark, J. H. *Chem. Rev.* **1980**, *80*, 429.
(29) Emsley, J. *Chem. Soc. Rev.* **1980**, *9*, 91.
(30) Liotta, C. L.; Harris, H. P. *J. Am. Chem. Soc.* **1974**, *96*, 2250.
(31) Neumann, P.; El-Kohli, A.; Müller, U.; Dehnicke, K. *Z. Anorg. Allg. Chem.* **1989**, *577*, 185.
(32) Christe, K. O.; Wilson, W. W.; Wilson, R. D.; Bau, R.; Feng, J. *J. Am. Chem. Soc.* **1990**, *112*, 7619.
(33) Kiriazis, L.; Mattes, R.; Obst, F. *Inorg. Chim. Acta* **1991**, *181*, 157.
(34) Chisholm, M. H.; Clark, D. L.; Huffman, J. C. *Polyhedron* **1985**, *4*, 1203.

Table V. Data for 13 $Mo_2X_4(PR_3)_4$ Compounds As Shown in Figure 3

	compound	δ–δ^*, nm	LMCT, nm	ref
a	$Mo_2F_4(PMe_3)_4$	550	283	this work
b	$Mo_2Cl_4(PMe_3)_4$	583	324	5
c	$Mo_2Cl_4(PEt_3)_4$	583	325	8
d	$Mo_2Cl_4(PBu^n_3)_4$	588	326	8, 10
e	$Mo_2Cl_4(PPr^n_3)_4$	590	325	8
f	$Mo_2Me_4(PMe_3)_4$	590	333	9a
g	$Mo_2Cl_4(PMe_2Ph)_4$	596	334	1
h	$Mo_2Br_4(PMe_3)_4$	598	345	5
j	$Mo_2Cl_4(PEt_2Ph)_4$	600	335	8
k	$Mo_2Cl_4(PMePh_2)_4$	600	350	8
m	$Mo_2Br_4(PPr^n_3)_4$	600	370	8
n	$Mo_2Br_4(PEt_3)_4$	610	385	8
o	$Mo_2I_4(PMe_3)_4$	633	395	4, 5

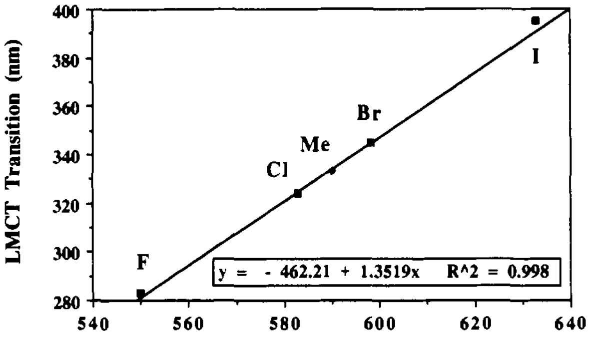

Figure 2. Plot of the LMCT transition vs the δ–δ^* transition for $Mo_2X_4(PMe_3)_4$ compounds where X = F, Cl, Me, Br, and I.

which such a disorder has been found, although it is encountered in various $Mo_2X_4(PR_3)_4$ compounds with R = Et, Pr, and Bu.[35]

In Table IV the dimensions of $Mo_2F_4(PMe_3)_4$ are compared with those for the $Mo_2X_4(PMe_3)_4$ molecules with X = Cl, Br, and I. The Mo–Mo distance, 2.110 (5) Å, may be slightly shorter, but on the 3σ criterion this cannot be asserted. The Mo–P distance, however, is clearly about 0.1 Å shorter than those in the other three compounds, and we do not believe that this could be an artifact arising from the disorder. We believe it happens because of the small size of the F atoms, which not only are closer to the Mo_2 core but also leave more room for the P atoms because they have a smaller van der Waals radius and the Mo–Mo–F angles are ca. 11° smaller than the other Mo–Mo–X angles. The Mo–Mo–P angle (104.6°) is not unusual compared to those (average 103.2°) in the other three compounds. The Mo–F distance, 2.105 (2) Å, appears normal in comparison to those in other compounds.[33,34,36–40]

Comparison of the $Mo_2X_4(PMe_3)_4$ (X = F, Cl, Br, I) Compounds. The numerical data for these four compounds are assembled in Table IV. In addition, Table V lists many other $Mo_2X_4(PR_3)_4$ compounds with R other than Me and gives the positions of their δ–δ^* and LMCT absorption bands. A number of linear regression analyses have been carried out to see how well various pairs of measured properties correlate over the series of compounds. The results are presented in Table VI, and it may be seen that the correlations are quite good, especially for the four PMe_3 compounds. The V_{ionic} values were calculated by taking the ionic radii of F, Cl, Br, and I (1.33, 1.84, 1.96, and 2.20 Å, respectively)[41] and inserting them into the formula $V_{ionic} = (4/3)\pi(r_{ionic})^3$; we will simply note that the covalent radii, atomic volume, and ionic radii give correlations (>85%) similar to those of V_{ionic}.

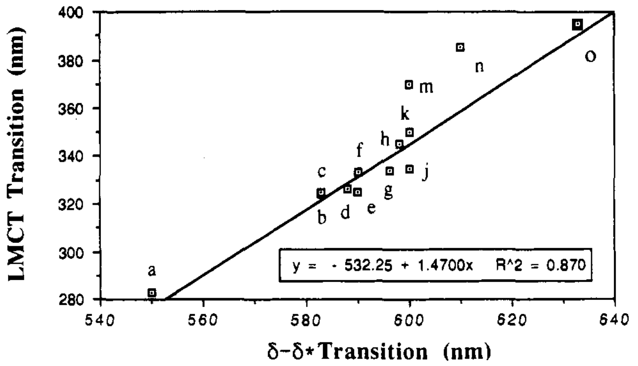

Figure 3. Plot of the LMCT transition vs the δ–δ^* transition for 13 $Mo_2X_4(PR_3)_4$ compounds.

One important result is that the δ–δ^* values correlate well with ϵ_{max}, Mo–X, V_{ionic}, and LMCT. As Figure 2 shows, the $Mo_2Me_4(PMe_3)_4$ complex also falls on the same line as the $Mo_2X_4(PMe_3)_4$ (X = F, Cl, Br, I) complexes; the tetramethyl compound was not included in the linear regression analysis. However, the $Mo_2X_4(PMe_3)_4$ (X = NCS, NCO) complexes which have δ–δ^* and LMCT transitions at 670, 395 nm and 617, 330 nm respectively, are way off the line. We find this surprising since the NCS and NCO ligands are usually considered pseudohalides. However, here they appear to have a very different effect on the δ and/or δ^* orbitals. In Figure 3, one can see the fair correlation of the δ–δ^* and LMCT transitions of the 13 compounds listed in Table V; it should be noted that the values used in the correlations are from both solution and Nujol mull data, which may contribute to the low correlation coefficient.

We now turn to the usefulness of these correlations. The correlations have been extended to the $Mo_2X_4(PEt_3)_4$, $Mo_2X_4(PPr^n_3)_4$ and $Mo_2X_8^{4-}$ complexes. In Table VI, parts C–E show the correlations between V_{ionic} and δ–δ^* and between V_{ionic} and LMCT, respectively. To find the predicted values for the δ–δ^* and LMCT bands of $Mo_2F_4(PEt_3)_4$, one simply uses V_{ionic} of fluoride (9.86) to obtain predicted values of 502 and 145 nm, respectively. The δ–δ^* value appears reasonable, but the LMCT transition is far too low. If one uses the predicted δ–δ^* value of 502 nm in the equation from Figure 3, the LMCT transition is calculated as 206 nm, which is more reasonable, but still too low. The predicted values are listed in Table VII. In Table VIE, parameters for the plot of δ–δ^* vs V_{ionic} for $Mo_2Cl_8^{4-}$ and $Mo_2Br_8^{4-}$ complexes are listed, where the δ–δ^* transitions are 513 and 556 nm, respectively. In a similar fashion one can predict the values for the δ–δ^* transition for $Mo_2F_8^{4-}$ and $Mo_2I_8^{4-}$ as 385 and 659 nm, respectively. It is difficult to estimate the errors in these values, but they may give at least a rough idea of what to expect for these compounds.

We turn finally to a discussion of the intensities of the δ–δ^* transition. It has been proposed elsewhere[5] that there is considerable mixing between the δ–δ^* transition and the π(ligand)–δ^*(Mo_2) transition. However, the previously proposed extent of this mixing may not be correct. In Table VIII we have tabulated some calculations which estimate the possible percent of mixing of the π(ligand)–δ^*(Mo_2) transitions. In the earlier work,[5] the "inherent" intensity of the δ–δ^* transition (i.e., that which could be attributed to a purely metal-based transition) was estimated to be about 150 M^{-1} cm^{-1}. We have considered three possible levels of inherent δ–δ^* transition intensity. In case A, the inherent intensity is given a generous value of 300. One can see from column 5 that in this case the percentage of the δ–δ^* transition's intensity stolen from the LMCT does in fact increase from F to

---

(35) Cotton, F. A.; Jennings, J. G.; Price, A. C.; Vidyasagar, K. *Inorg. Chem.* **1990**, *29*, 4138. In Table IX of this reference, it is incorrectly stated that $Mo_2Cl_4(PEt_3)_4$ shows ligand as well as metal disordering. Only $Re_2Cl_4(PEt_3)_4$ shows such complete disorder.

(36) Edwards, A. J.; Slim, D. R.; Guerchais, J. E.; Kergoat, R. *J. Chem. Soc., Dalton Trans.* **1977**, 1966.

(37) Crabtree, R. H.; Hlatky, G. G.; Holt, E. M. *J. Am. Chem. Soc.* **1983**, *105*, 7302.

(38) Burgmayer, S. J. N.; Templeton, J. L. *Inorg. Chem.* **1985**, *24*, 2224.

(39) Chisholm, M. H.; Clark, D. L.; Errington, R. J.; Folting, K.; Huffman, J. C. *Inorg. Chem.* **1988**, *27*, 2071.

(40) Hidai, M.; Kodama, T.; Sato, M.; Harakawa, M.; Uchida, Y. *Inorg. Chem.* **1976**, *15*, 2694.

(41) Shannon, R. D. *Acta Crystallogr.* **1976**, *A32*, 751.

Table VI. Tabulation of Correlation Coefficients and Equation Parameters of the Form $y = mx + b$

x	y	correlation	m	b
A. $Mo_2X_4(PMe_3)_4$ (X = F, Cl, Br, I)				
δ–δ^*, nm	Mo–X, Å	98.5	7.899×10^{-3}	−2.212
δ–δ^*, nm	V_{ionic}, Å^3	99.3	0.4163	−218.0
δ–δ^*, nm	LMCT, nm	99.8	1.352	−462.2
δ–δ^*, nm	ϵ_{max}, M^{-1} cm^{-1}	98.7	38.88	-1.935×10^4
LMCT, nm	ϵ_{max}, M^{-1} cm^{-1}	98.8	28.76	−6058
V_{ionic}, Å^3	LMCT, nm	98.5	3.214	246.7
Mo–X, Å	LMCT, nm	97.4	167.8	−75.42
X radius (covalent), Å	Mo–X, Å	99.8	1.064	1.345
V_{ionic}, Å^3	Mo–X, Å	99.6	1.901×10^{-2}	1.924
^{31}P NMR, ppm	^{1}H NMR, ppm	99.8	-5.183×10^{-2}	0.9820
atomic no.	^{31}P NMR, ppm	97.2	−0.1427	−7.039
atomic no.	^{1}H NMR, ppm	96.9	7.390×10^{-3}	1.347
B. The 13 Compounds Listed in Table V				
δ–δ^*, nm	LMCT, nm	87.0	1.470	−532.2
C. $Mo_2X_4(PEt_3)_4$ (X = Cl, Br)				
V_{ionic}, Å^3	δ–δ^*, nm	100[a]	4.958	453.6
V_{ionic}, Å^3	LMCT, nm	100[a]	11.017	37.52
D. $Mo_2X_4(PPr^n_3)_4$ (X = Cl, Br)				
V_{ionic}, Å^3	δ–δ^*, nm	100[a]	1.836	542.1
V_{ionic}, Å^3	LMCT, nm	100[a]	8.263	109.4
E. $Mo_2X_8^{4-}$ (X = Cl, Br)				
V_{ionic}, Å^3	δ–δ^*, nm	100[a]	7.896	307.0

[a] These correlations = 100, since there are only two values being used in the calculation.

Table VII. Predicted Values of the δ–δ^* and LMCT Transitions for Various Complexes

complex	δ–δ^*, nm	LMCT, nm
$Mo_2F_4(PEt_3)_4$	502	145 (206)[a]
$Mo_2I_4(PEt_3)_4$	675	529 (460)[a]
$Mo_2F_4(PPr^n_3)_4$	560	191 (291)[a]
$Mo_2I_4(PPr^n_3)_4$	624	478 (385)[a]
$Mo_2F_8^{4-}$	385	
$Mo_2I_8^{4-}$	659	

[a] The values in parentheses are calculated from the equation in Figure 3.

I, in good agreement with the results of Hopkins et al.[5] The amount of stolen intensity appears to be very large and would indicate a large amount of mixing. However, these values in column 5 may be deceptive. Since one can see from column 2 that there is a large increase in the intensity of the LMCT transition down the column, the actual percentage of stolen intensity (column 6) appears to be large for X = F and much less for X = I. The same conclusions can be drawn from cases B and C, for which we have set the inherent intensity at 1000 for case B and 2090 for case C, where it is assumed that there is no mixing for the fluoride.

We agree that the δ–δ^* transition borrows intensity from the LMCT band, but the results in Table VIII do not support the view that there is an "increase in the extent of mixing between the δ–δ^* and π(ligand)–δ^*(Mo_2) transitions". In fact, it appears that the percentage of mixing can actually decrease as one proceeds from F to I, depending upon the assumed amount of inherently metal-based contribution to the intensity. The significant increase in the δ–δ^* transition intensity is perhaps more likely to be the result of the increasing intensity of the LMCT band and not to be due to an increase in the amount of mixing. In other words, it is not that the δ–δ^* transition progressively borrows a higher percentage from the LMCT but, rather, that the intensity of the LMCT increases dramatically down the series. It is difficult to place a value on the "inherent" intensity of the δ–δ^* transition, as it may well vary, not only from one series to another [$Mo_2(O_2CCR_3)_4$ vs $Mo_2X_4(PR_3)_4$] but even within one series such as the one we have discussed.

Concluding Remarks. Apart from the intrinsic interest of the $Mo_2F_4(PR_3)_4$ compounds, we would like to call attention to the method by which they were prepared. We believe that the reaction

Table VIII. Calculations for the Percentages of Mixing for $Mo_2X_4(PMe_3)_4$ Species

X	1 δ–δ^* ϵ_{max}, M^{-1} cm^{-1}	2 LMCT ϵ_{max}, M^{-1} cm^{-1}	3 inherent δ–δ^* intensity, M^{-1} cm^{-1}	4[a] amt of δ–δ^* intensity stolen from LMCT, M^{-1} cm^{-1}	5[b] % of δ–δ^* intensity stolen from LMCT	6[c] δ–δ^* intensity stolen as a % of LMCT
Case A						
F	2090	2110	300	1790	85.6	84.4
Cl	3110	3720	300	2810	90.4	75.5
Br	4060	6650	300	3760	92.6	56.5
I	5250	11850	300	4950	94.3	41.8
Case B						
F	2090	2110	1000	1090	52.2	51.6
Cl	3110	3720	1000	2110	56.7	56.7
Br	4060	6650	1000	3060	75.4	46.0
I	5250	11850	1000	4250	81.0	35.9
Case C						
F	2090	2110	2090	0.0	0.0	0.0
Cl	3110	3720	2090	1020	32.8	27.4
Br	4060	6650	2090	1970	48.5	29.6
I	5250	11850	2090	3160	60.2	26.7

[a] Column 4 = column 1 − column 3. [b] Column 5 = (column 4/column 1) × 100. [c] Column 6 = (column 4/column 2) × 100.

of Olah's reagent with organometallic compounds could afford a much-needed, efficient general route to transition metal fluoro complexes. There is a vast array of starting materials, but few reagents useful for making M–F bonds. Neither in a recent review[42] nor in our own examination of the literature could we find any precedent for the employment of Olah's reagent to convert metal–alkyl to metal–fluorine bonds. We proffer the suggestion that Olah's reagent may also be useful for the conversion of M–OR or M–H bonds to M–F bonds, whereby ROH or H_2, respectively, would be released.

Acknowledgment. We thank the National Science Foundation for support and Dr. Patrick M. Killough of Shell Development Co. for the Raman data.

Registry No. **1**, 138630-82-7; **2**, 138630-83-8; $Mo_2Me_4(PMe_3)_4$, 64376-69-8; $Mo_2Me_4(PMe_2Ph)_4$, 67619-18-5; Mo, 7439-98-7.

Supplementary Material Available: A table of anisotropic thermal parameters (1 page); a listing of structure factors (1 page). Ordering information is given on any current masthead page.

---

[42] Doherty, N. M.; Hoffman, N. W. *Chem. Rev.* **1991**, *91*, 553.

Contribution from the Arthur Amos Noyes Laboratory, California Institute of Technology, Pasadena, California 91125, and Department of Chemistry and Biochemistry, University of California, Los Angeles, Los Angeles, California 90024

Spectroelectrochemistry of Copper–Zinc Superoxide Dismutase

Cynthia Strong St. Clair,[†] Harry B. Gray,*[,†] and Joan Selverstone Valentine*[,‡]

Received August 12, 1991

The temperature dependence of the reduction potential of bovine copper–zinc superoxide dismutase (CuZnSOD) has been determined at pH 7.0, with potassium ferricyanide as the mediator. The following thermodynamic parameters were obtained: $E°' = 403 \pm 5$ mV vs NHE, $\Delta G°' = -9.31$ kcal/mol (pH 7.0, 25 °C, μ 0.1 M); $\Delta H°' = -21.4$ kcal/mol, $\Delta S°' = -40.7$ eu, $\Delta S°'_{rc} = -25.1$ eu. The large negative enthalpy of reduction may reflect the factors that are responsible for the unusually low reactivity of the enzyme with outer-sphere electron-transfer reagents.

Introduction

Bovine copper–zinc superoxide dismutase (CuZnSOD) is a dimeric enzyme of molecular weight 31 200 Da, containing one copper(II) and zinc(II) per monomer subunit.[1–4] According to the results of an X-ray crystal structure study of the oxidized (Cu^{II}) form of the enzyme at 2-Å resolution,[5–7] the copper site has a highly distorted square-pyramidal geometry with four histidine imidazoles and a water molecule as ligands, the latter occupying the apical position. One of the histidine imidazoles is deprotonated and acts as a bridging ligand between Cu^{II} and Zn^{II} in the nearby zinc site. The zinc site has a roughly tetrahedral geometry with the bridging imidazolate, two unshared histidine imidazoles, and an aspartate carboxylate making up the four ligands. The copper binding site in each monomer is located at the bottom of a narrow channel that is approximately 12 Å deep. Several charged residues on the surface of the protein and in the active-site channel appear to be important in directing superoxide and other anions toward the copper ion.[6,7] Catalysis of superoxide disproportionation occurs at the copper, which is accessible to solvent; the zinc ion seems primarily to play a structural role and is inaccessible to solvent.[1–4] The mechanism proposed for this enzyme involves reduction of Cu^{II} by one superoxide followed by oxidation of Cu^{I} back to Cu^{II} by a second superoxide. The Cu^{II} ions in the two subunits of the protein dimer are separated by 34 Å and appear to function independently.[1–4]

Reduction of the Cu^{II} form of CuZnSOD to give the Cu^{I} enzyme is accompanied by dissociation of the bridging imidazolate ligand from Cu^{II} and protonation of the nitrogen that had been bound to copper. That same ligand, now converted from imidazolate to imidazole, remains bound to zinc.[8] The reduction potential of CuZnSOD has been reported to be in the range 280–420 mV vs NHE.[9,10] In spite of this relatively high reduction potential, work in our laboratory has shown that CuZnSOD is reduced very slowly by reagents such as ascorbate and $Fe(CN)_6^{4-}$.[11] By contrast, the reaction of superoxide with either the oxidized or reduced form of CuZnSOD is known to occur with a rate near the diffusion limit.[12]

We undertook the study described here in order to characterize more fully the redox thermodynamics of CuZnSOD and to relate this new information to the observed kinetic properties. We used the technique of visible spectroelectrochemistry to measure the reduction potential and its temperature dependence, thereby determining the enthalpy and entropy of the reaction.[13] The results of this study are described here along with a discussion of how they may be related to the kinetics of the redox reactions of CuZnSOD.

Experimental Section

Materials. CuZnSOD isolated from bovine liver was purchased from Diagnostic Data, Inc. (Mountain View, CA). All other materials were prepared by standard procedures or used as supplied.[11]

Methods and Instrumentation. Long-path spectroelectrochemical measurements were performed by using 2-cm optical path length cells, prepared by minor modifications of a previously reported design.[14] The working electrode was a piece of gold foil that lines three walls of the sample compartment; the foil was connected by conducting epoxy to a gold wire, which acted as the external contact. The working electrode compartment was 7.2-mm wide by 16.0-mm high. Potentials were applied with a Princeton Applied Research polarographic analyzer (Model 174A) and measured with a microvolt digital multimeter (Keithley 177). The reference electrode was a miniature SCE (Sargent-Welch), and the counter electrode was a platinum wire. Sample solutions were stirred during electrochemical equilibration via a pneumatic stirrer contained

---

[†] California Institute of Technology.

[‡] University of California, Los Angeles.

(1) Valentine, J. S.; Pantoliano, M. W. In *Metal Ions in Biology*; Spiro, T. G., Ed.; Wiley-Interscience: New York, 1981; Vol. 3, Chapter 8, pp 291–358.
(2) Valentine, J. S.; Mota de Freitas, D. *J. Chem. Educ.* **1985**, *62*, 990–997.
(3) Bannister, J. V.; Bannister, W. H.; Rotilio, G. *Crit. Rev. Biochem.* **1987**, *22*, 111–180.
(4) Oberley, L. W., Ed. *Superoxide Dismutase*; CRC Press: Boca Raton, FL, 1982; Vols. I and II.
(5) Tainer, J. A.; Getzoff, E. D.; Beem, K. M.; Richardson, J. S.; Richardson, D. C. *J. Mol. Biol.* **1982**, *160*, 181–217.
(6) Tainer, J. A.; Getzoff, E. D.; Richardson, J. S.; Richardson, D. C. *Nature* **1983**, *306*, 284–287.
(7) Getzoff, E. D.; Tainer, J. A.; Weiner, P. K.; Kollman, P. A.; Richardson, J. S.; Richardson, D. C. *Nature* **1983**, *306*, 287–290.
(8) Bertini, I.; Luchinat, C.; Monnanni, R. *J. Am. Chem. Soc.* **1985**, *107*, 2178–2179.
(9) Fee, J. A.; DiCorleto, P. E. *Biochemistry* **1973**, *12*, 4893–4899.
(10) Lawrence, G. D.; Sawyer, D. T. *Biochemistry* **1979**, *18*, 3045–3050.
(11) St. Clair, C. S. Ph.D. Thesis, California Institute of Technology, 1989.
(12) Klug-Roth, D.; Fridovich, I.; Rabani, J. *J. Am. Chem. Soc.* **1973**, *95*, 2786–2790.
(13) Taniguchi, V. T.; Sailasuta-Scott, N.; Anson, F. C.; Gray, H. B. *Pure Appl. Chem.* **1980**, *52*, 2275–2281.
(14) Ellis, W. R. Ph.D. Thesis, California Institute of Technology, 1986.